https://doi.org/10.31436/iiumej.v25i2.3211

GEOMETRIC QUALITY ANALYSIS OF TERRESTRIAL LASER SCANNING DATA FOR INDUSTRIAL USAGE

ALI SALAH J. AL-SAEDI [1,2*], FANAR M. ABED [3], IMZAHIM A. ALWAN [2]

[1] *Surveying Department, Amara Technical Institute, Southern Technical University, Misan, Iraq*
[2] *Civil Engineering Department, University of Technology, Baghdad, Iraq*
[3] *Surveying Engineering Department, College of Engineering, University of Baghdad, Baghdad, Iraq*

**Corresponding author: ali.alsaedi@stu.edu.iq*

(Received: 4 March 2024; Accepted: 28 June 2024; Published online: 15 July 2024)

ABSTRACT: Terrestrial laser scanning is a potential emerging technology increasingly used in several applications, including reverse engineering, digital reconstruction, deformation monitoring, forensic crime scene preservation, and construction (AEC) applications. The data tolerance accepted in these applications ranges from tens of millimeters (e.g., historical monument digitization) to tens of micrometers (e.g., industrial high-precision manufacturing and assembling). Instrument mechanism, atmospheric conditions, object surface characteristics, and scan geometry are the four main factors that affect the laser point clouds produced by the Time of Flight (TOF) 3D laser scanner. Consequently, research groups worldwide have put a significant effort into modeling the sources of TOF-TLS errors and design-specific performance evaluation methodologies. This paper investigated the influence of scanning geometry parameterized by incidence angle and the range on the quality of TOF-TLS data in industrial sites. The quality of an indoor sample dataset of an industrial case study was studied and assessed. The results showed that the incidence angle and range parameters substantially impacted the quality of the TOF-TLS data. The suggested methodology can accurately correct the laser data to eliminate the incidence angle and range effects. A revised and optimized point cloud dataset was reconstructed by utilizing these features in conjunction with the approximated quality of the individual points. Furthermore, when assessing the quality of individual point clouds, the accuracy validation obtained through the RMSE value was 3 mm based on ground-truth reference points. On the other hand, the standard deviation values computed through the Multi-Scale Model-to-model cloud (M3C2) analysis were revealed to reach 1mm, which shows better performance results than the Cloud-to-Cloud (C2C) and Cloud-to-Model (C2M) comparison analysis. However, the proposed method may result in the elimination of several significant laser points. These points of high incidence angle values are not eliminated in every instance. The effect of scanning geometry, represented by the angle of incidence with the normalized intensity of the scanning points, should be studied intensively in future studies.

ABSTRAK: Terestrial pengimbas laser adalah teknologi yang berpotensi besar dalam pelbagai aplikasi, termasuk kejuruteraan balikan, rekonstruksi digital, pengawasan perubahan bentuk, pemeliharaan tempat kejadian jenayah forensik, dan aplikasi konstruksi (AEC). Penerimaan data toleransi dalam aplikasi ini adalah dalam julat lingkungan beberapa milimeter (cth: digitalisasi monumen sejarah) sehingga beberapa mikrometer (cth: industri pembuatan berkejituan tinggi dan pemasangan). Mekanisme alatan, keadaan atmosfera, ciri-ciri permukaan objek, dan geometri pengimbas adalah empat faktor utama yang memberi kesan terhadap gumpalan asap titik laser terhasil daripada masa terbang (TOF) 3D pengimbas laser. Oleh itu, kumpulan pengkaji sedunia telah berusaha bersungguh-sungguh dalam pemodelan sumber ralat TOF-TLS dan mereka kaedah penilaian prestasi reka bentuk tertentu. Kajian ini dipengaruhi oleh geometri pengimbas berparameter sudut tuju dan julat kualiti data

TOF-TLS dalam kawasan industri. Kualiti sampel set data dalam bangunan menggunakan kajian pembelajaran industri telah diteliti dan dinilai. Dapatan kajian menunjukkan sudut tuju dan julat parameter sangat mempengaruhi kualiti data TOF-TLS. Kaedah yang dicadangkan ini dapat memperbetulkan arah secara tepat iaitu kesan pengurangan sudut tuju dan julat. Set data rawak titik yang diubah dan dioptimumkan telah dibina semula dengan menggunakan ciri-ciri ini bersempena kualiti anggaran titik-titik individu. Tambahan, apabila menaksir kualiti titik rawak individu, pengesahan ketepatan yang diperoleh melalui nilai RMSE dijumpai sebanyak 3 mm berdasarkan titik-titik panduan kesahihan bumi. Di samping itu, nilai sisihan piawai yang dikira melalui analisis Model-ke-model Skala-Pelbagai Rawak (M3C2) didapati mencapai 1 mm, di mana menunjukkan dapatan prestasi lebih baik berbanding analisis Rawak-ke-rawak (C2C) dan Rawak-ke-Model (C2M) secara bandingan. Walau bagaimanapun, kaedah yang dicadangkan ini mungkin menyebabkan penyisihan beberapa titik laser penting. Titik-titik ini yang mempunyai nilai sudut tuju yang tinggi adalah tidak disisihkan pada setiap masa. Kesan pengimbas geometri, merupakan sudut tuju dengan keamatan ternormal titik-titik pengimbas, perlu dikaji dengan lebih lanjut pada masa depan.

KEYWORDS: *Terrestrial Laser Scanning, Industrial, Quality Analysis, Scanning Geometry, Range, Incidence Angle.*

1. INTRODUCTION

In the last two decades, Terrestrial Laser Scanners have become frequently used systems in reverse engineering and the quality control of facilities and infrastructures [1–3]. TLS device advantages include fast acquisition possibilities, sizeable spatial coverage, and high measurement accuracy [4]. Using a spherical coordinate system, the TLS provides a three-dimensional scene visualization by measuring the distances to the surfaces of the scanned objects. In addition to recording a horizontal and vertical angle for each point, it also measures the range from the hit point on the surface to the scanner location [5]. Noise affects scan measurements, even though TLS measurements are precise. Ultimately, point cloud measurements contain both systematic and random unavoidable errors. During data pre-processing stages, such as registration or segmentation, spread errors of individual points are propagated into end products, such as 3D reconstructions [6,7]. Individual point quality is influenced by four main factors: (i) the mechanism of the scanner, (ii) the atmospheric conditions and environment, (iii) the properties of the object being scanned, and (iv) the scanning geometry [5,8]. All of the factors affect the measurement of individual points, potentially by introducing noise or by altering the intensity and shape of the signal that is being emitted. There are many factors over which the user has limited control, such as the scanner, the atmospheric, and the object properties. The only component the user may control is the scanning geometry, as the user can decide where the scan should take place and, as a result, the perspective from which a point cloud is viewed [5]. In addition, when discussing the data, precision, outliers, and other incorrect points must be considered. Therefore, it is necessary to identify and eliminate untrusted points and outliers from the dataset or follow an adjustment procedure to clean the data for further accuracy analysis and more robust measurement data [5].

Scanning geometry is defined by the range and the point incidence angle computed to a surface [5]. This factor is well studied and investigated in Airborne Laser Scanning data [9–11]. On the other hand, the scanning geometry of the TLS data has been studied in numerous studies. For instance, in the investigation of intensity return using a variety of scanning geometry settings, the effects of range and incidence angle on the intensity measurements of (TLS) have been analyzed by Kaasalainen et al. [12], who investigated correction methods for

various TLS instruments and targets. Other studies by Tan and Cheng [13] suggested a new way to eliminate these range and incidence angle effects on the TLS intensity data. This method is based on linear interpolation of intensity values from reference targets. In this context, Pesci and Teza [14] designed an experiment to investigate the effect of surface irregularities on intensity data, depending on the TLS survey. This experiment involved acquiring TLS-based data depending on a rotating artificial target with flat and irregular surfaces. The results showed that the differences in the intensity of the backscattered signal depend on surface type and the incidence angle. Some previous studies proposed various strategies and modeled for eliminating the influence of inappropriate scan geometry on TLS data. Soudarissanane et al. [5] focused on understanding the influence of scan geometry on the quality of individual points in a point cloud, specifically the local measurement noise. Following this, the study successfully modeled the dependence of measurement noise on distance and incidence angle for planar surfaces. Later studies investigated the influence of incidence angle on the precision of terrestrial laser scanning points, where they could identify and correct the noise due to incidence angle, along with other influencing factors, to provide a better measurement quality [15]. Moreover, Pardiñas et al. [3] hypothesized a methodology for building an error model of TLS measurements using object distances and incidence angles. A point cloud of a tunnel section is used to analyze the spatial distribution of errors. The error model is applied in this case. The findings demonstrated that the point density, as a surface fitted to the point cloud, counteracts the angle of incidence's impact on the point cloud quality close to the tunnel gable. Miriam et al. [16], discussed the influence of incidence angle (IA) on TLS distance measurements. They developed a new methodology for comparing TLS distances measured directly with reference distances. The study proved that at close range, other error effects were more pronounced than the influence of IA. On the other hand, the systematic effect of IA at a distance of about 30 m, was obviously recorded. The effect of the scanning geometry is used in many studies, for example, model deformation in man-made structures [3,17] as well as objects in natural sites that use scanning geometry constraints [18–20].

This paper discusses the analysis, assessment, and correction of 3D point clouds generated by terrestrial laser scanning systems for industrial applications. The paper examines the effects of the scanning geometry on the point cloud's quality, focusing especially on the laser beam's incidence angle and range in relation to industrial sites. Furthermore, we looked at the feasibility of assessing a single point's quality. The measurements' received signal level steadily decreases as the incidence angle and range are raised. The paper is structured as follows: Section 2 details the techniques employed. The case study is described in Section 3. The results and discussion are presented in Section 4, and the conclusions are provided in Section 5.

2. METHODS

2.1 Scanning Geometry

The ultimate output of a scan is frequently a point cloud with n observations, each containing the 3D coordinates $[x_i, y_i, z_i]$, where $i = 1, \dots, n$ of a point in the Cartesian coordinate system. The scanner can detect the signal reflected from a surface using the TLS as the coordinate system's center. The two directional angles are then recorded: the vertical angle, or latitude, or φ_i, and the horizontal angle, or longitude, or θ_i. It calculates the distance ρ_i to the reflection's surface. The scanning geometry can impact the point cloud's quality, including the incidence angle and range. For this reason, evaluating and reducing errors and uncertainties in TLS data requires an awareness of the consideration of the scanning geometry [4]. This research defined the surface local orientation in 3D space based on point cloud geometry in a local coordinate system where the vector $P_i = [x_i, y_i, z_i]$ where $i = 1, \dots, n$, defined by a

https://doi.org/10.31436/iiumej.v25i2.3211

specific neighboring radius value [20]. The angle between the normal vector N of the surface and one laser beam vector Pi is called the incidence angle αi, as shown in Figure 1. For more information, see Eq. (1) [10,15].

$$\alpha i = cos^{-1}\left(\frac{Pi \cdot N}{|Pi||N|}\right) \quad (1)$$

The unit vector that points outward and is perpendicular to the surface's tangent plane at Pi is called the normal vector N. Consequently, the incidence angle is always in the interval [0 < αi < 90]. When a perpendicular laser beam strikes a surface, the resulting footprint is expected to be circular. Otherwise, the footprint will get more eccentric and elongated as the incidence angle increases. Their magnitude is proportional to the ellipse's major and minor axes [21].

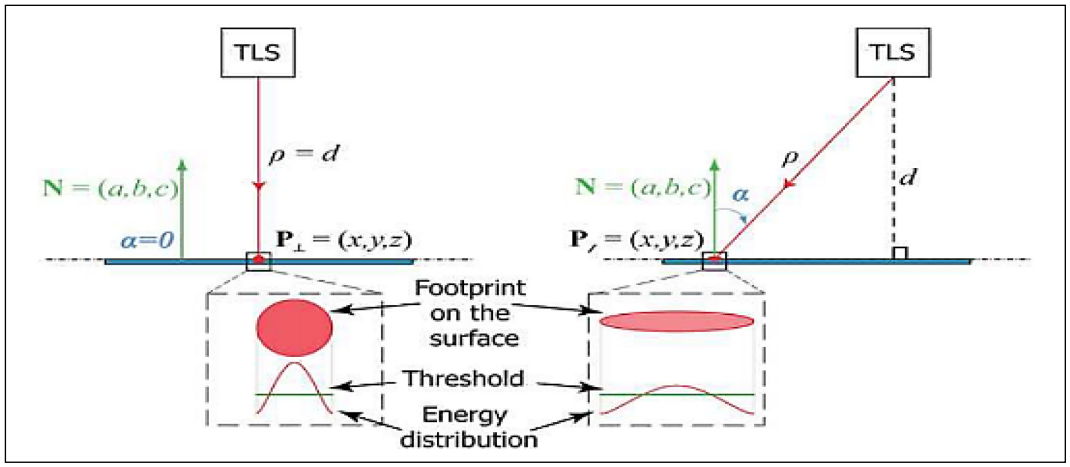

Figure 1. Diagram depicting the reflection geometry.

The TLS technology allows precise surface-to-object distance measurements by sending out laser beams in predetermined angular orientations and measuring the reflected signals in the same direction [5]. This research calculates the effect of scanning geometry depending on the radar range equation, see Eq. (2). It is defined as a function of the scanning geometry [22].

$$P_R(\rho) = P_T \frac{D_R^2 \chi \cos\alpha}{4\rho^2} \eta_{sys}\eta_{atm} \quad (2)$$

In the system settings, P_R is received power and P_T is transmitted power, and they are measured in watts, ρ is the range of the laser beam in meters, D_R is the diameter of the receiver aperture in meters, χ is the cross-section of the target, and η_{sys} and η_{atm} are the transmission factors in the system and the atmosphere, respectively. The SNR of a laser return decreases as the cosine of the incidence angle α increases, as shown in Eq. (2). Additionally, the degradation of SNR is inversely proportional to the square of the range [5].

2.2 Analyzing the Laser Point Quality

The assumption of planar surfaces illustrates the quality of the individual points that make up a point cloud. The estimation method known as total least squares [5], is utilized in this paper to acquire planar features.

2.2.1 Accuracy (Geometric) Analysis

The accuracy is an absolute value and is defined as the mean deviation of the measured coordinates from their reference values. To determine the accuracy coordinates from high-definition TLS, target scans are used with their equivalent 3D points (GCPs and CPs), which are calculated using an accurate reference technique. Geometric accuracy refers to how well

https://doi.org/10.31436/iiumej.v25i2.3211

point clouds match actual or ground-truth data. The 3D coordinate's accuracy can be expressed by Root Mean Square Error (RMSE), as stated in Eq. (3). In this equation, the variable V represents the difference between a measured value and its ground truth value. In contrast, the variable n represents the total number of observations [23–27].

$$RMSE = \pm\sqrt{\frac{\sum_{i=1}^{n} v_i^2}{n}} \quad (3)$$

2.2.2 Precision (Physical) Analysis

In a TLS system, the deviation of a sample of measurements from the mean value is a measure that can be used to determine the precision of individual measurements [28]Through its definition, the standard deviation of an LS plane can be defined as a reference value for a single measurement of noise. Various analyses were utilized to identify and verify the 3D point cloud quality by comparing them to the reference models. These methods included roughness analysis, C2C distance analysis, C2M distance analysis, and M3C2 comparison.

2.2.2.1 Roughness Analysis

Most Time of Flight (TOF) scanners are susceptible to noise (or roughness) during range collection. Point cloud roughness can be measured by computing the distance between each point and the best-fitting plane calculated to its nearest neighbors [29]. Cloud Compare (CC) software (https://www.cloudcompare.org) presents flexible tools where roughness is computed by specifying the radius of a sphere centered on individual points [19, 29].

2.2.2.2 Cloud-to-Cloud Distance (C2C) Analysis

This method is the quickest and easiest direct method for comparing three-dimensional point clouds. This method requires no data gridding, meshing, or surface normal calculation procedures. It is possible to determine the surface change most straightforwardly by calculating the distance between the two points (C2C, Figure 2A). There are two ways in which the local reference surface model can be improved: first, by employing a height function (C2C_HF, Figure 2B), and second, by using a least square fit of the closest point neighbors [30]. Cloud matching algorithms like the ICP also take advantage of this method. However, as shown in Figures 2A and 2B, the spacing of the points, outliers, and roughness of the clouds all impacted the distance measurement [19].

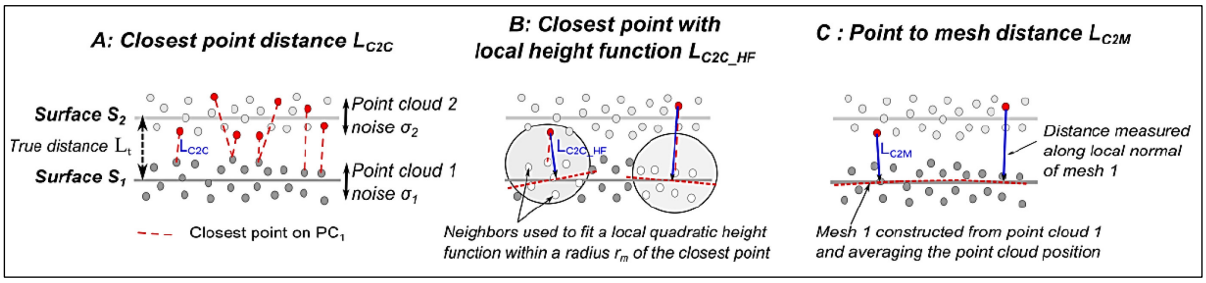

Figure 2. Current 3D comparison techniques for evaluating the similarities and differences between two data points, PC1 and PC2 [19].

2.2.2.3 Cloud to Mesh Distance (C2M) Analysis

This method is the one that is used the most commonly to analyze point cloud precision levels. The distance between a point cloud and a reference three-dimensional theoretical model or mesh determines how much surface change is detected [31,32]. This method is useful for flat surfaces because it allows one to build a mesh that corresponds to the average position of the reference point cloud (Figure 2C). On the other hand, the process of creating surface

https://doi.org/10.31436/iiumej.v25i2.3211

meshes is made more difficult either by point clouds that have a significant amount of roughness across all scales or by missing data related to occlusion. In most cases, a manual inspection that takes a lot of time has to be performed. In addition, mesh construction helps to smooth out specific details that may be significant when evaluating the properties of the local roughness [19].

2.2.2.4 Multi-scale Model to Model Cloud (M3C2) Analysis

The M3C2 approach determines the cloud to cloud distance between the two compared models. Instead of using traditional algorithms' random nearest neighbor distance, the M3C2 method calculates the distance along a local normal direction based on the surface's roughness. This method is better at dealing with point location uncertainty and registration errors. It is possible to provide a general description of the M3C2 algorithm by breaking it down into four steps, as illustrated in Figure 3. Step one begins with selecting the core points used in the reference model. The software then determines each core point's normal direction using a fitting plane under the control of a set of normal scales *D*. In the next step, the projection depth *h* and projection scale *d* of the cylinder will be modified to generate a cylinder that is aligned along the normal direction that is already known. Step three involves separating the three-dimensional model-derived sets of points inside the cylinder into their respective sets. Finally, the distance between two subsets of points is calculated using the average position length along the normal direction. Lague et al. [19] provide a more detailed description of the M3C2 algorithm for further details.

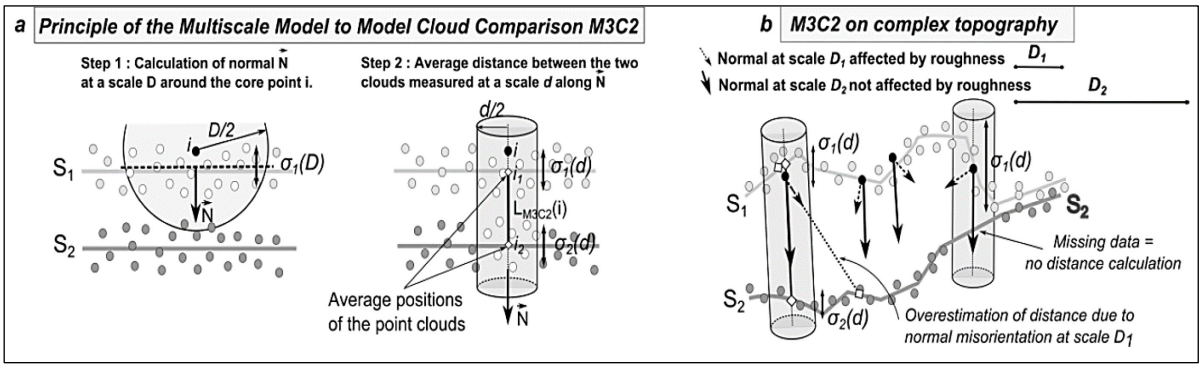

Figure 3. The M3C2 technique calculates the distance between clouds [19].

3. CASE STUDY

The quality analysis approaches described in section 2 are applied in this study using point cloud datasets obtained from the STONEX X300 terrestrial laser scanner. This device was used to collect 3D data in a controlled environment to examine the impact of scanning geometry on the resulting scan quality and analyze the quality of individual points. The scanner is a pulse-detection device that contains two integrated cameras with a resolution of 5 megapixels each. It has a range accuracy of less than 5mm at 50 meters [33]. Figure 4 shows the Area of Interest (AOI) industrial device, which is a SATO SATRONIK C3250 Plasma Cutting Machine fabricated in Germany. It is known for its intricate design and small details used for cutting thin and thick materials. This technology is widely used in industries like fabrication and metalworking for fast and accurate cutting.

https://doi.org/10.31436/iiumej.v25i2.3211

Figure 4. Plasma cutting machine case study.

The site should be planned carefully to achieve actual scanning, as well as determine the optimal scanning positions and targeting locations. The distribution of artificial targets over and surrounding the machine facilitates the alignment of the point clouds acquired from various stations. These targets were used for geo-referencing, the connection of individual scans (registration), and assessing the 3D accuracy of the coordinate measurements obtained from TLS. The trajectory positions were not spacious enough for circle scanning, even though the point clouds were obtained from fifteen scan positions about 3–4 m away from the machine.

The main goal of post-processing is to achieve clean and registered point clouds. Most processing operations for laser point clouds are carried out by JRC 3D Reconstructor 3, which is a native software provided by STONEX (https://www.stonex.it). The process of aligning data from various scans into one common coordinate system is called data registration. JRC 3D-Reconstroctor involves two types of automatic registration: pair-wise (ICP) and global (LM-ICP). LM-ICP with Bundle Adjustment was adopted to refine the alignment, as it allows the registration of all the scans and evenly distributes the registration error. Model alignment was performed before executing the C2C, C2M, and M3C2 methods, as demonstrated in Figure 5.

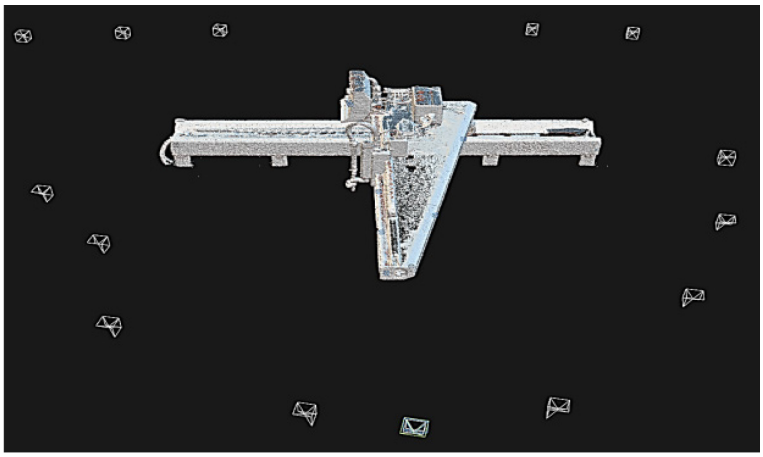

Figure 5. Registered TLS data scans of SATO SATRONIK C3250.

4. RESULTS AND DISCUSSION

4.1 Quality assessment based -geometric and physical aspects

As mentioned, fifteen stations were captured for the regular geometry point cloud. The precision assessment was applied to the plasma cutting machine case study to evaluate the laser scan measurements and eliminate outliers. According to Section 2.2.2, analysis is used to assess individual points' quality. Results are illustrated in Figures 6 and 7, where (a) refers to

https://doi.org/10.31436/iiumej.v25i2.3211

roughness analysis, (b) refers to C2C analysis, (c) refers to C2M analysis, and (d) refers to M3C2 analysis. The precision assessment was applied to a real dataset with outliers, as shown in Figure 6. As a next step, the precision assessment was applied to a dataset without outliers, see Figure 7. The quality analysis methods are carried out using the CC software. In Figure 6, the grey and red points on the bottom of the machine represent the invalid outlier point cloud, mainly because the corresponding points cannot be detected using the small projection scale in the C2C, C2M, and M3C2 methods.

CC contains several filters, including SOR filter and Noise filter, which are applied to remove noise and outliers from the data in this study. In the SOR filter, 6 points were used to estimate the mean distance, while in the noise filter, the k-D tree (k-dimensional tree) value was set at 6 points, and the radius was selected to 0.01 m to include neighbors. Compact spatial data structures like k-D trees are ideal for significant tasks like determining the location of nearby neighbors. Each node in the k-D tree is used to split up one of the k dimensions in a binary search tree. However, some outliers cause deformation even when applied above filters. Therefore, they were removed manually from the target point cloud to simulate the occlusion regions, whose roughness is shown in Figure 6 (a). Whereas the standard deviation of roughness in the datasets with outlier values was equal to 1.2 mm, noting that the local neighborhood radius was set at 0.01 m. However, it was noticed in Figure 7 (a) that the standard deviation was decreased to approximately 0.6 mm when removing the outliers due to a decrease in the local neighborhood radius of 0.005 m. The roughness values are widely dispersed as the outliers are present, according to the Gaussian roughness distribution.

According to C2C analysis, the standard deviation of datasets that include outliers was 0.077 m, Figure 6 (b). Compared with Figure 7 (b), the standard deviation dropped to 0.006 m as the outliers were removed. However, this method can be used only for calculating the relative distance between corresponding points without reflect of signed displacement. On the other hand, a reflection of the change in the direction of the point cloud can be carried out using C2M analysis, as it generates sharp triangles easily when constructing the mesh and TIN model. This is not suitable for complex scanning scenes. Figure 6 (c) and Figure 7 (c) showed the similarities of the standard deviation values for both C2M and C2C methods, which was 0.075 m in the dataset, including outliers, compared to 0.012 m without outliers. To calculate the quality, the M3C2 analysis is performed where Figure 6 (c) indicates the analysis results for the datasets with outliers, as the projection depth was 0.406 m. Obviously, the neighborhood normal vector and initial projection radius are set at 0.1 m and 0.05 m, which are determined according to the point cloud surface roughness. On the other hand, using the M3C2 method, Figure 7 (c) shows the quality analysis results of the datasets without outliers. The projection depth of the latter was 0.407 m, and the normal vector neighborhood and initial projection radius were set to 0.094 m and 0.047 m, respectively. For a comparison between Figure 6(c) and Figure 7(c), a variation has been noticed in the standard deviation with projection depth using the M3C2 according to the Gaussian distribution of roughness, specifically, at the depths 16 and 20 cm, as the maximum standard deviations were 0.006 m and 0.001 m, respectively. It can be concluded that the M3C2 analysis can be used to obtain more accurate quality results compared to C2C and C2M methods.

https://doi.org/10.31436/iiumej.v25i2.3211

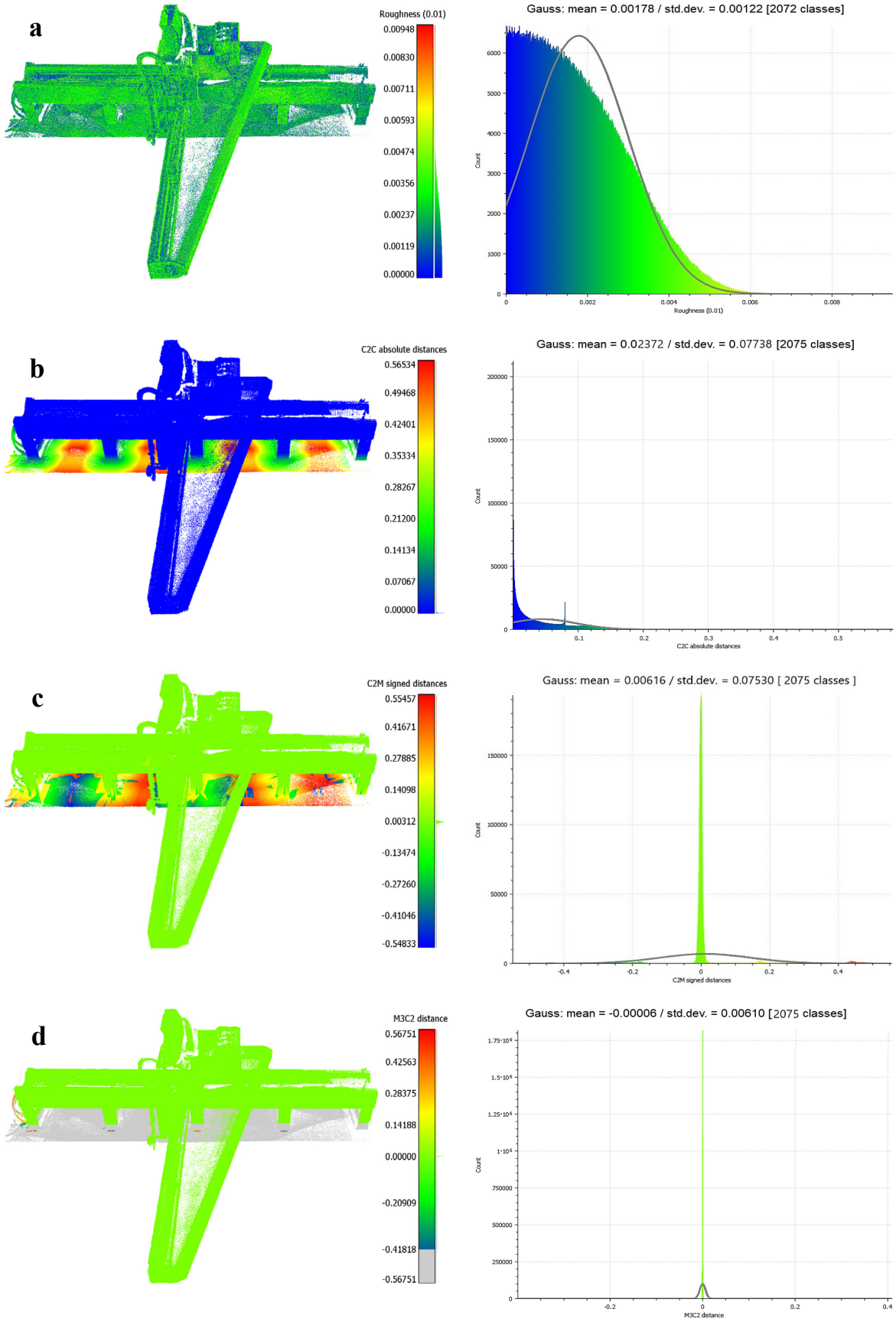

Figure 6. Real dataset of the plasma cutting machine with outliers analysis (a) Roughness, (b) C2C, (c) C2M, and (d) M3C2

https://doi.org/10.31436/iiumej.v25i2.3211

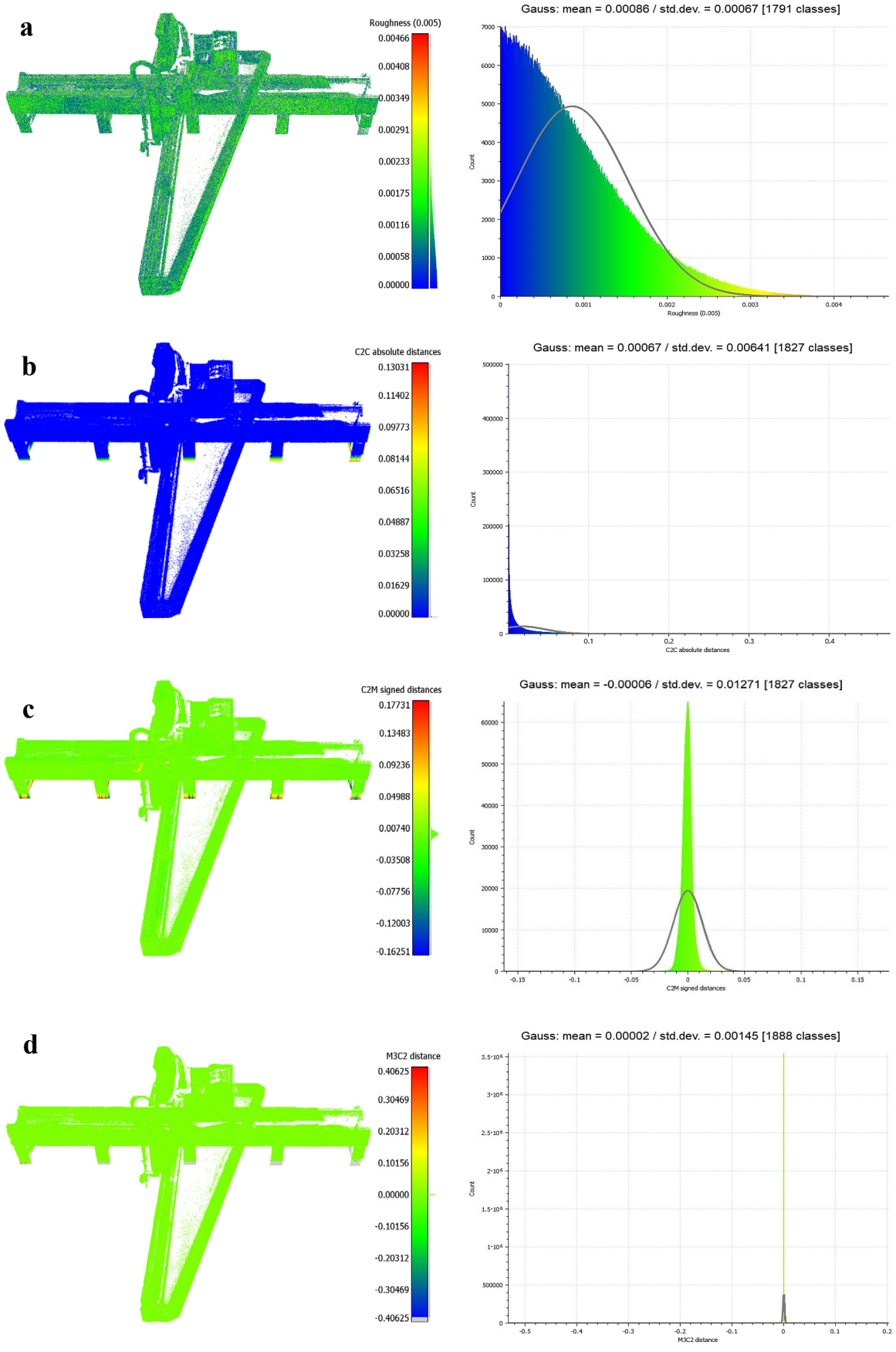

Figure 7. Real dataset of the plasma cutting machine without outliers analysis (a) Roughness, (b) C2C, (c) C2M, and (d) M3C2

https://doi.org/10.31436/iiumej.v25i2.3211

Analysis of the outcome of the results from applied algorithms has been performed to understand how outliers affect data variability, Table 1. As an advantage, this analysis contributes to a precise understanding of the underlying patterns in each parameter and directs researchers in making appropriate decisions about data pre-processing and interpretation. Depending on the results obtained from the current study, we found that the M3C2 method outperformed the C2C and C2M methods for the deformation analysis. Figure 8 illustrates the data standard deviations with and without outliers using the mentioned analysis methods. An increase in standard deviation values indicates that the involvement of outliers will increase data variability. Once outliers are removed from a dataset, the standard deviation values drop, bringing the remaining values closer to the mean. Since outliers may distort statistical metrics, researchers often eliminate outliers for better comprehension of data's underlying trends and patterns.

Table 1. Compares the real dataset before and after outlier removal in different analysis methods.

Case Study	**Real Dataset with Outliers**			**Real Dataset without Outliers**		
No. of Points	**4301853**			**3334525**		
Method	**Classes**	**Mean (m)**	**Std. Dev. (m)**	**Classes**	**Mean (m)**	**Std. Dev. (m)**
Roughness	2072	0.00178	0.00122	1791	0.00086	0.00067
C2C	2075	0.02372	0.07738	1827	0.00067	0.00640
C2M	2075	0.00616	0.07530	1827	0.00006	0.01271
M3C2	2075	0.00006	0.00610	1888	0.00002	0.00145

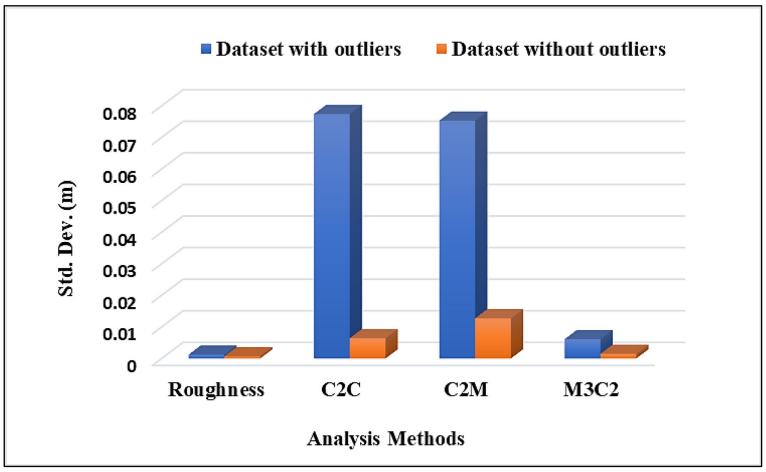

Figure 8. Compares the entire dataset standard deviations with and without the presence of outliers.

Figure 9 illustrates a selected part of the case study machine, (a) and (b) indicate the evaluation quality of TLS data with and without the presence of outliers, respectively. The choice of this part is based on containing small and complex details and estimating the effectiveness of previous evaluation analysis methods depending on the size and other details of the case study. Different results are obtained according to the analysis methods utilized and are similar to those obtained in the entire case study, as shown in Table 2. In addition to having lower highest and lowest standard deviation values, 0.008 m and 0.003 m, respectively, than other approaches, the M3C2 method has demonstrated its efficacy by producing valuable and accurate quality analysis data when compared to the C2C and C2M methods. Refer to Figure 10 for additional clarification.

https://doi.org/10.31436/iiumej.v25i2.3211

Table 2. Compares dataset of part (1) before and after outlier removal using different analysis methods.

Part 1	Real Dataset with Outliers			Real Dataset without Outliers		
No. of Points	732599			490218		
Method	Classes	Mean (m)	Std. Dev. (m)	Classes	Mean (m)	Std. Dev. (m)
Roughness	853	0.00172	0.00124	681	0.00087	0.00068
C2C	856	0.03070	0.06900	701	0.00109	0.00681
C2M	856	0.01038	0.08713	701	0.00052	0.01928
M3C2	856	0.00002	0.00820	701	0.00011	0.00335

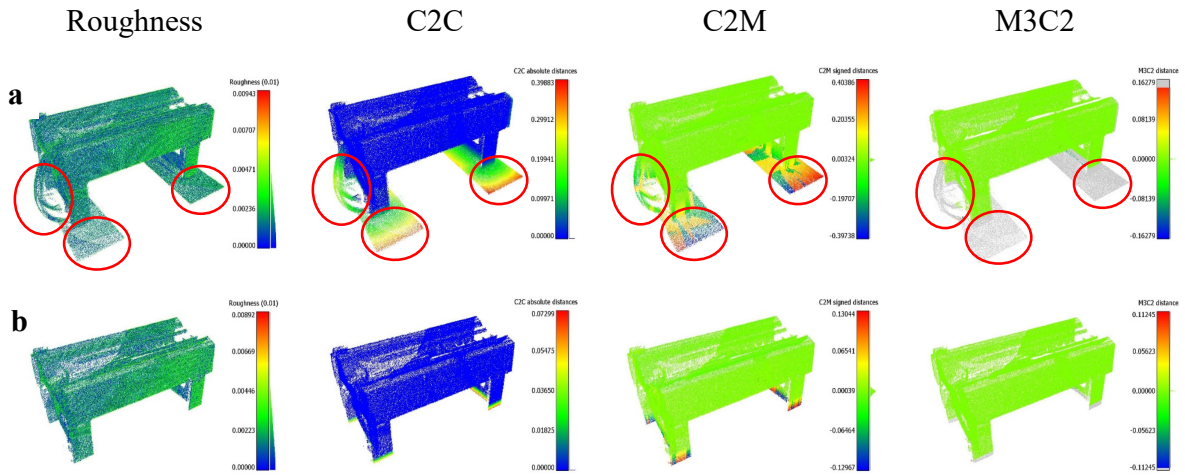

Figure 9. Dataset of the selected part from plasma cutting machine (a) with the presense of outliers, (b) without the presense of outliers, using different analysis methods.

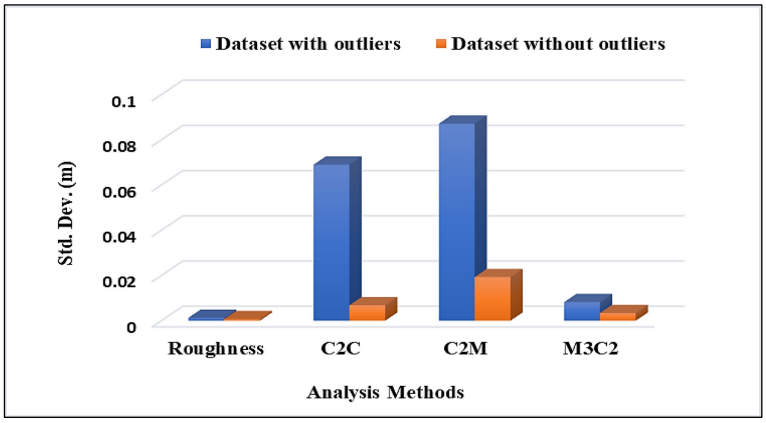

Figure 10. Compares the dataset of the selected part standard deviations with and without outliers.

On the other hand, the point clouds produced by laser scanners often contain numerous points that exhibit significant inaccuracies caused by various variables. Therefore, a geometric evaluation was used to evaluate the laser scan measurements for the plasma cutting machine case study. This was implemented by calculating the RMSE and comparing the results with the values of the associated GCPs and CPs in the laser point cloud. To ensure that TLS point clouds are geometrically accurate, we survey a selection of GCPs and CPs using a total station reference device. The RMSE values delivered from the selected GCPs and CPs were 2.9 mm and 3.2 mm, respectively, as illustrated in Table 3. We can notice that the errors were delivered

in the x direction. However, the largest error was targeted at points 3 and 6. This can be justified due to the position of points 3 and 6, which were covered by only 3 scans, while 5 scans covered other points.

4.2 Quality assessment based -scanning geometry

Two tests are carried out using data from the plasma cutting machine to examine the influence of scanning geometry parameters such as range and incidence angle on the quality of the computed point clouds. The first test was implemented to determine the effect of different ranges per point on the point cloud quality. According to the laser range equation, Eq. (2), the quantity of power received decreases as the scan range increases.

Table 3. RMSE-based control points and checkpoints.

NO.	Type	X error (m)	Y error (m)	Z error (m)	Total error (m)	RMSE
1	Control Point	0.0026	0.0027	0.0016	0.0028	0.0029
2	Control Point	0.0013	0.0011	0.0025	0.0021	
3	Control Point	0.0036	0.0021	0.0027	0.0033	
4	Control Point	0.0028	0.0017	0.0031	0.0030	
5	Check Point	0.0029	0.0021	0.0027	0.0030	0.0032
6	Check Point	0.0030	0.0025	0.0033	0.0035	
7	Check Point	0.0018	0.0017	0.0012	0.0029	

The range's impact on the overall noise level grows as the square of the range does. This outcome can be demonstrated in Figure 11. The range values are illustrated through the horizontal axis, and the standard division is illustrated through the vertical axis. Assuming a constant incidence angle, the standard deviation alters as a function of scanning distance. Compared to other ranges, the point cloud quality registered a lower standard deviation value at the 9-meter range. It has a high-precision standard deviation of 0.006 m for roughness, while M3C2 has a standard deviation of 0.007 m. The degree of detail was maintained by ensuring that all sections and intricacies of the machine were covered completely.

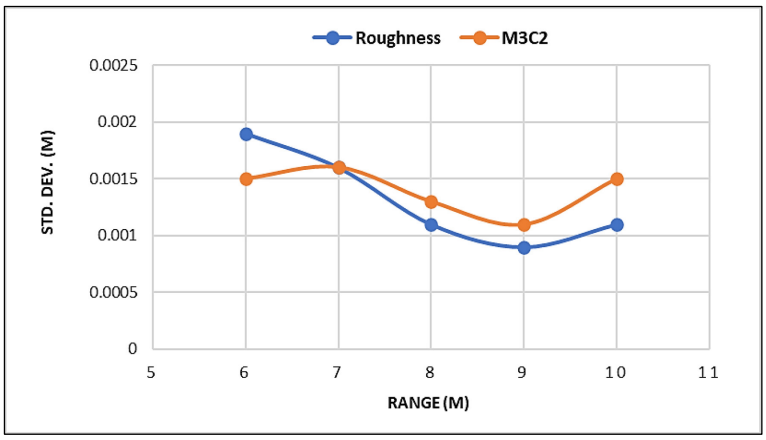

Figure 11. Experiments of range effects on the point cloud quality.

On the other hand, the second experiment was applied to examine the effect of the incidence angle on the range measurement. The scanning distance from the TLS to the experimental plasma-cutting machine was 9 m. As shown in Figure 12, the point cloud quality is observed as the laser incidence angle varies from 0° to 90° in 10° increments.

https://doi.org/10.31436/iiumej.v25i2.3211

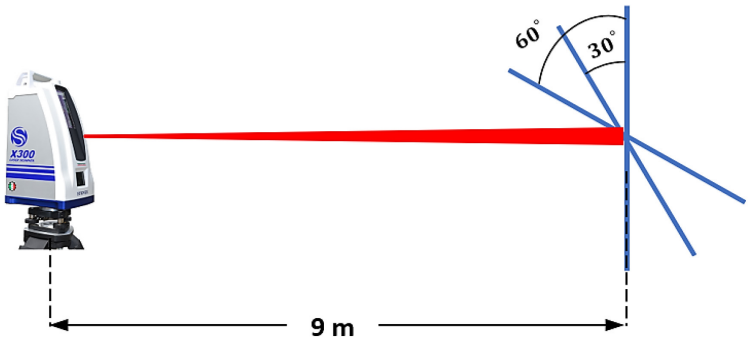

Figure 12. Measurement setup of the incidence angle experiments.

The incidence angles were calculated based on Eq. (1) and using Cyclone 3DR software. Table 4. provides information on the total number of original case study points and the percentage of points filtered at different incidence angles. As the incidence angle increases, the percentage of filtered points generally decreases. For example: At an incidence angle of 10°, 92.4% of the original points have been filtered. This trend continues, and the percentage of the filtered points decreases as the incidence angle increases. No points have been screened at a 90-degree incidence angle (0.00%). Specific data points may be deemed less reliable or credible at lower incidence angles if a higher percentage of points are filtered at those angles.

Table 4. Number and percentage of points filtered at different incidence angles.

Total No. of original case study 1883731 points	**Points have been filtered**	
Incidence angle (°)	**No. of points**	**percentage**
10	1740226	92.4%
20	1511891	80.3%
30	1384072	73.5%
40	1328672	70.5%
50	1292664	68.6%
60	1255326	66.6%
70	1143550	60.7%
80	653468	34.7%
90	0	0.00%

For further explanation, Figure 13 visually represents the relationship of filtered points with different incidence angles. The points in red represent the remaining points at any specific angle, while the remaining points of blue color will be filtered. In addition, Figure 14 illustrates a net-view analysis of the plasma cutting machine with the incidence angles and the number or density of points to demonstrate this effect in different ranges.

Finally, the effect of the incidence angle was calculated for roughness and M3C2 analysis methods. Figure 15 shows the impact of the incidence angle on the quality of the point cloud at individual points, as indicated in Eq. (2), using the estimated planar parameters per segment. As the incident angle increases, the point cloud quality diminishes when the scanning distance remains constant. The point cloud quality is relatively consistent and close together, especially when the angle falls between 0° and 60°. However, it drops if the incident angle is greater than 60 degrees. When the angle hits 80 degrees, achieving the necessary measurement accuracy becomes more difficult [10,34]. This can be explained by calculating the effect of the incidence angle on the measurement according to the range equation Eq. (2), the function cos α. As the angle of incidence increases, the deterioration of the signal increases, which it is directly

https://doi.org/10.31436/iiumej.v25i2.3211

proportional and also due to the dispersion behavior of the different surfaces with respect to the incoming light [5,35]. Figure (15) displays the standard deviation as it changes with the change of the incident angle. Figure 16 and Figure 17 also show how the point cloud quality changes as a function of incidence angle. The degradation of the measurement precision is particularly pronounced for darker-colored angles.

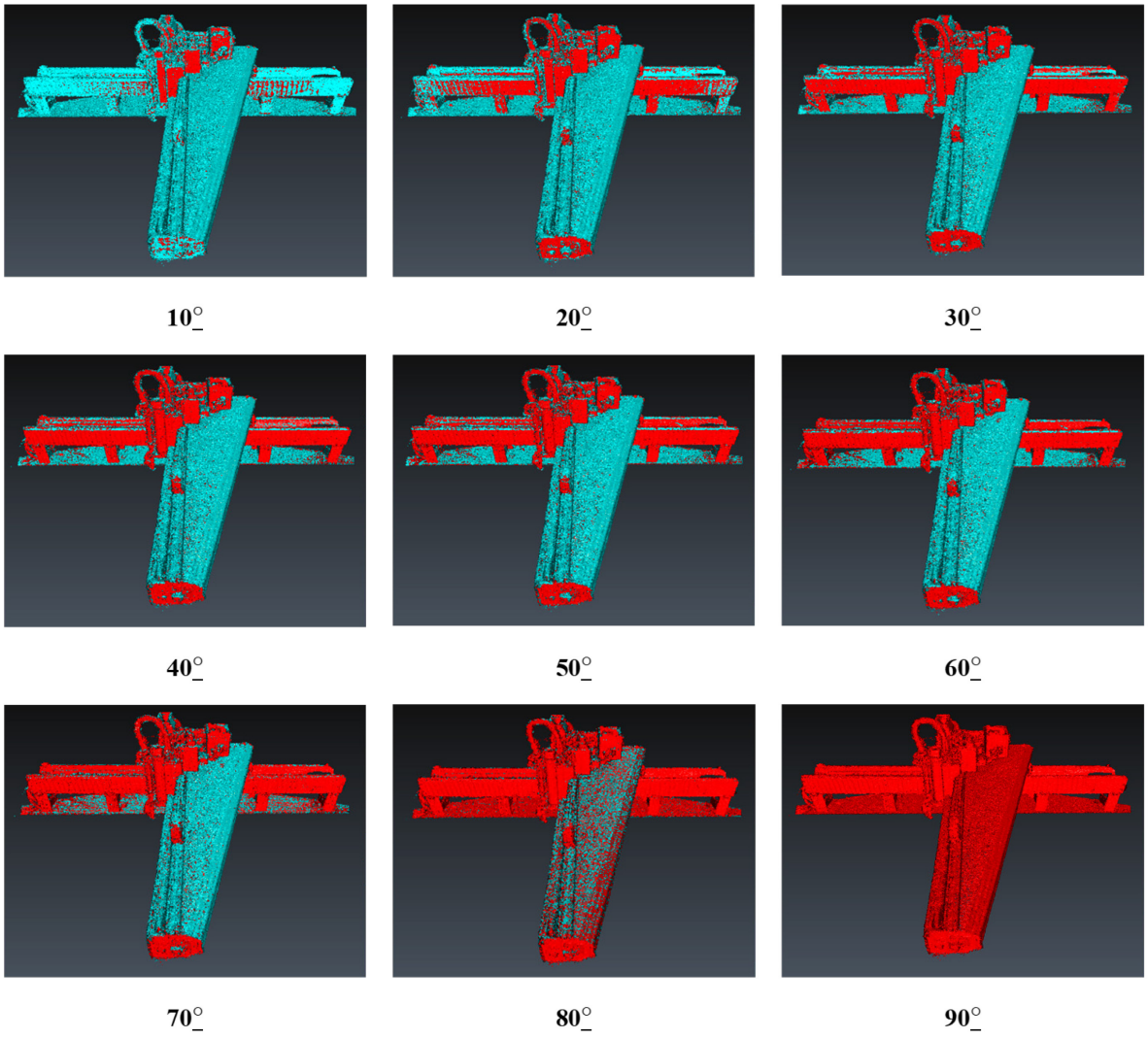

Figure 13. Point clouds of the plasma cutting machine colored with different incidence angles.

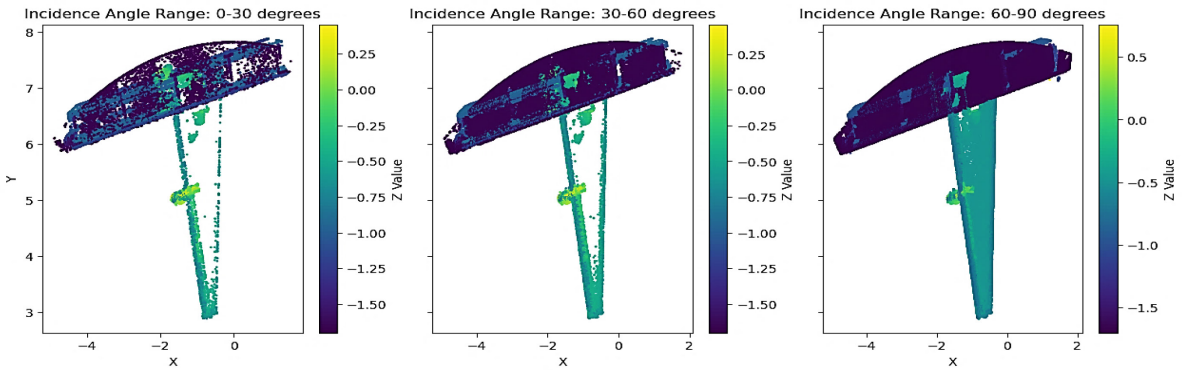

Figure 14. Net-view of the plasma cutting machine with the incidence angles.

https://doi.org/10.31436/iiumej.v25i2.3211

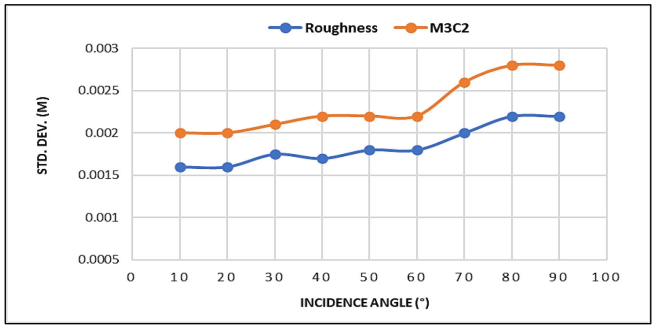

Figure 15. Experiments of incidence angles effects on the point cloud quality.

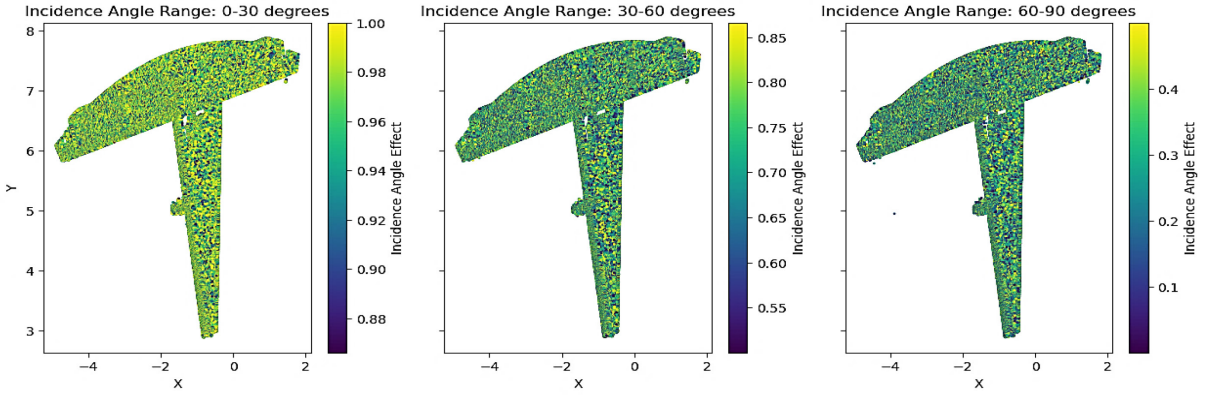

Figure 16. Net-view of the plasma cutting machine with the incidence angle effects.

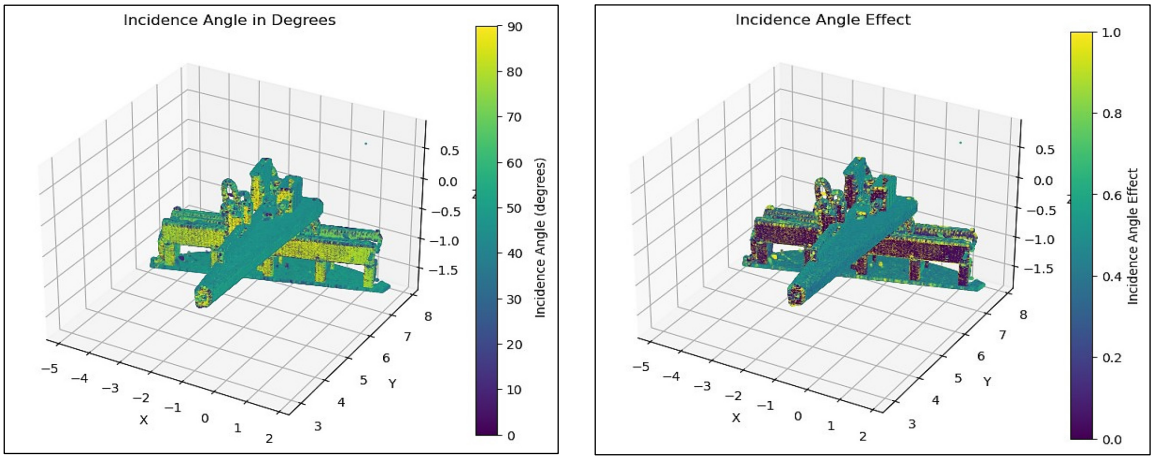

Figure 17. Three Three-dimensional net-views of the plasma cutting machine colored with (a) incidence angles and (b) incidence angle effects.

5. CONCLUSION

This paper presents a workable solution for improving laser point cloud quality in complicated situations by analyzing the impact of scanning geometry, such as incidence angle and range, for industrial applications. The paper also discusses the quality assessment of laser point clouds based on geometric and physical aspects. This includes analyzing the results of multiple statistical analyses in indoor standard conditions. Recognizing and minimizing the effects of these impacts is of the utmost importance for the 3D reverse engineering industry. The proposed method demonstrates a high degree of simplicity and accuracy for laser point cloud analysis.

Quantifying the quality of the point cloud is accomplished by a geometrical analysis of its accuracy. Using RMSE as a metric for evaluation, this study investigated the RMSE value for CPs as 0.003 meters, while for GCPs, it was 0.002 meters. Quantify analysis can be performed by precision analysis, which is also known as physical analysis. Standard deviation is used as a measurement of the evaluation. CC tools are utilized to analyze the roughness, C2C, C2M, and M3C2 approaches. Each approach has advantages and disadvantages, as illustrated by [36]. Hence, this method is robust to changes in point density and point cloud noise. Deformation analysis results proved the efficiency of the M3C2 method compared to C2C, C2M, and roughness methods [19]. The effect of outliers on data variability can be understood by comparing datasets with and without their presence, specifically focusing on the standard deviations. For each parameter's values, removing outliers and extreme values from the dataset generates a dataset more representative of the normal distribution. This approach assists scholars in making a proper decision whenever they are preparing and interpreting their data, as it provides a more detailed picture of the patterns that occurred for each parameter. Assessment of point cloud quality based on scanning distance and laser incidence angle. Regarding the effect of scanning geometry on the signal-to-noise ratio, it is possible to estimate the increased measurement noise due to increasing incidence angle and range. The findings indicate that terrestrial laser scanners with a minor beam divergence can collect high-accuracy point clouds over longer scanning distances if the laser incident angle is less than 60 degrees. However, a point cloud quality analysis must be performed before multi-station registration, as the scanning distance and angle change depending on the origin of the computed coordinates.

The point cloud quality has a substantial relationship with the criteria discussed above for accurate applications such as industrial engineering. By optimizing the incidence angles and ranges of the laser scanning data capture, it is possible to ascertain more stable data and a better-quality positioning outcome. Consequently, it will be feasible to lessen the overall error associated with the measurements using more sophisticated scenarios in future studies.

ACKNOWLEDGEMENT

The authors give their heartfelt thanks to the Head of the Photogrammetry and Laser Scanning Laboratory in the Department of Surveying Engineering, University of Baghdad, for providing the laser scanning device and related data collection tools and the needed technical support. It is also necessary to acknowledge the engineering workshop in the College of Engineering to facilitate collecting the data and working in the study area.

REFERENCES

[1] Tang P, Huber D, Akinci B, Lipman R, Lytle A. (2010). Automatic reconstruction of as-built building information models from laser-scanned point clouds: A review of related techniques. Automation in construction, 19(7): 829-843.

[2] Teza G, Pesci A. (2013). Geometric characterization of a cylinder-shaped structure from laser scanner data: Development of an analysis tool and its use on a leaning bell tower. Journal of Cultural Heritage, 14(5): 411-423.

[3] Roca-Pardiñas J, Argüelles-Fraga R, de Asís López F, Ordóñez C. (2014). Analysis of the influence of range and angle of incidence of terrestrial laser scanning measurements on tunnel inspection. Tunnelling and underground space technology, 43: 133-139.

[4] Vosselman, G., and Maas, H. G. (2010). Airborne and Terrestrial Laser Scanning. CRC press.

[5] Soudarissanane S, Lindenbergh R, Menenti M, Teunissen P. (2011). Scanning geometry: Influencing factor on the quality of terrestrial laser scanning points. ISPRS journal of photogrammetry and remote sensing, 66(4): 389-399.

[6] Muralikrishnan B. (2021). Performance evaluation of terrestrial laser scanners—A review. Measurement Science and Technology, 32(7): 072001.

[7] Thamir ZS, Abed FM. (2020). How geometric reverse engineering techniques can conserve our heritage; a case study in Iraq using 3D laser scanning. In IOP Conference Series: Materials Science and Engineering, 737(1): 012231.
[8] Jurek T, Kuhlmann H, Holst C. (2017). Impact of spatial correlations on the surface estimation based on terrestrial laser scanning. Journal of Applied Geodesy, 11(3): 143-155.
[9] Schaer P, Skaloud J, Landtwing S, Legat K. (2007). Accuracy estimation for laser point cloud including scanning geometry. In Mobile Mapping Symposium 2007, Padova.
[10] Abed FM, Mills JP, Miller PE. (2012). Echo amplitude normalization of full-waveform airborne laser scanning data based on robust incidence angle estimation. IEEE Transactions on Geoscience and Remote Sensing, 50(7): 2910-2918.
[11] Kaasalainen S, Ahokas E, Hyyppa J, Suomalainen J. (2005). Study of surface brightness from backscattered laser intensity: Calibration of laser data. IEEE Geoscience and Remote Sensing Letters, 2(3): 255-259.
[12] Kaasalainen S, Jaakkola A, Kaasalainen M, Krooks A, Kukko A. (2011). Analysis of incidence angle and distance effects on terrestrial laser scanner intensity: Search for correction methods. Remote Sensing, 3(10): 2207-2221.
[13] Tan K, Cheng X. (2016). Correction of incidence angle and distance effects on TLS intensity data based on reference targets. Remote Sensing, 8(3): 251.
[14] Pesci A, Teza G. (2008). Effects of surface irregularities on intensity data from laser scanning: an experimental approach. Annals of Geophysics.
[15] Soudarissanane S, Lindenbergh R, Menenti M, Teunissen, P., & Delft, T. (2009). Incidence angle influence on the quality of terrestrial laser scanning points, ISPRS. In Proceedings ISPRS Workshop Laser scanning (pp. 1-2).
[16] Zámečníková M, Neuner H, Pegritz S, Sonnleitner R. (2015). Investigation on the influence of the incidence angle on the reflectorless distance measurement of a terrestrial laser scanner. Iulia Dana Negula, Violeta Poenaru, 37.
[17] Khalaf AZ, Al-Saedi ASJ. (2016). Assessment of Structure with Analytical Digital Close Range Photogrammetry. Engineering and Technology Journal, 34(11): 2140-2151.
[18] Milenković M, Pfeifer N, Glira P. (2015). Applying terrestrial laser scanning for soil surface roughness assessment. Remote sensing, 7(2): 2007-2045.
[19] Lague D, Brodu N, Leroux J. (2013). Accurate 3D comparison of complex topography with terrestrial laser scanner: Application to the Rangitikei canyon (NZ). ISPRS journal of photogrammetry and remote sensing, 82: 10-26.
[20] Hussein LY, Alwan IA, Ataiwe TN. (2023). Smart city 3D modeling with a total station and a smartphone. In IOP Conference Series: Earth and Environmental Science (Vol. 1129, No. 1, p. 012002).
[21] Sun W, Wang J, Yang Y, Jin F, Sun F. (2023). Accurate deformation analysis based on point position uncertainty estimation and adaptive projection point cloud comparison. Geocarto International, 2175916.
[22] Höfle B, Pfeifer N. (2007). Correction of laser scanning intensity data: Data and model-driven approaches. ISPRS journal of photogrammetry and remote sensing, 62(6): 415-433.
[23] Luhmann T, Robson S, Kyle S, Harley I. (2011). Close range photogrammetry: Principles, techniques and applications.
[24] Khalaf AZ, Ataiwe T, Mohammed I, Kareem A. (2018). 3D Digital modeling for archeology using close range photogrammetry. In MATEC Web of Conferences (Vol. 162, p. 03027). EDP Sciences.
[25] Hadi AH, Khalaf AZ. (2022). Accuracy Assessment of Establishing 3D Real Scale Model in Close-Range Photogrammetry with Digital Camera. Engineering and Technology Journal, 40(11): 1492-1509.
[26] Hussein LY, Alwan IA, Ataiwe TN. (2023). Evaluation of the accuracy of direct georeferencing of smartphones for use in some urban planning applications within smart cities. In AIP Conference Proceedings, 2793 (1).
[27] Khalaf AZ, Alwan IA, Jameel A. (2013). Establishment oF 3D Model with Digital Non-Metric Camera in Close Range Photogrammetry. Engineering and Technology Journal, 40(11): 1492-

1509
[28] Wunderlich TH, Wasmeier P, Ohlmann-Lauber J, Schäfer TH, Reidl F. (2013). Objective specifications of terrestrial laserscanners–A contribution of the geodetic laboratory at the Technische Universität München. Lehrstuhl für Geodäsie.
[29] CloudCompare forum [https://www.cloudcompare.org/forum/]
[30] Girardeau-Montaut D, Roux M, Marc R, Thibault G. (2005). Change detection on points cloud data acquired with a ground laser scanner. International Archives of Photogrammetry, Remote Sensing and Spatial Information Sciences, 31 (8): 1601-1611.
[31] Monserrat O, Crosetto M. (2008). Deformation measurement using terrestrial laser scanning data and least squares 3D surface matching. ISPRS Journal of Photogrammetry and Remote Sensing, 63(1): 142-154.
[32] Olsen MJ, Kuester F, Chang BJ, Hutchinson TC. (2010). Terrestrial laser scanning-based structural damage assessment. Journal of Computing in Civil Engineering, 24(3): 264-272.
[33] JRC 3D Reconstructor stonex [https://www.stonex.it/project/x300-laser-scanner/]
[34] Abed FM, Mills JP, Miler PE. (2014). Calibrated full-waveform airborne laser scanning for 3D object segmentation. Remote Sensing, 6(5): 4109-4132.
[35] Lichti DD. (2008). A method to test differences between additional parameter sets with a case study in terrestrial laser scanner self-calibration stability analysis. ISPRS Journal of Photogrammetry and Remote Sensing, 63(2): 169-180.
[36] Teng J, Shi Y, Wang H, Wu J. (2022). Review on the Research and Applications of TLS in Ground Surface and Constructions Deformation Monitoring. Sensors, 22(23): 4109-4132.